Proc. Natl. Acad. Sci. USA
Vol. 79, pp. 5327–5331, September 1982
Cell Biology

Dependence of locally measured cellular deformability on position on the cell, temperature, and cytochalasin B

(cytoskeleton/mechanical properties/cytotensiometer/microfilaments)

NILS O. PETERSEN, WILLIAM B. MCCONNAUGHEY*, AND ELLIOT L. ELSON

Department of Biological Chemistry, Washington University School of Medicine, St. Louis, Missouri 63110

Communicated by Robert L. Baldwin, June 10, 1982

ABSTRACT **We describe an approach to exploring cell surface–cytoskeleton interactions through direct measurements of the mechanical resistance of living cells to locally applied forces. These measurements are sensitive to variations in structure across the cell and at various depths below its surface. We find that local cellular deformability depends on the temperature and on the integrity of the cytoskeleton. Cytochalasin B increases the deformability of all regions of the cell except the nucleus.**

The shape of an adherent animal cell in culture results from a balance of forces applied to its plasma membrane from within by the cytoskeleton and from without by the extracellular matrix. Dynamic cellular functions such as locomotion, phagocytosis, and cytokinesis require changes of shape driven by contractile cytoskeletal machinery containing actin microfilaments. The biochemical mechanisms by which contractile forces are generated are presumed to be similar in muscle and nonmuscle cells (1, 2). In muscle cells, microfilaments are collectively and stably anchored in Z-disks and dense bodies. In nonmuscle cells such as fibroblasts, some microfilaments, organized into bundles or stress fibers, may be similarly anchored into adhesion placques. In general, however, microfilament organization is transient and rearranges to meet changes in environment. Therefore, the means by which the forces generated by individual microfilaments are integrated to produce systematic changes of the shapes of nonmuscle cells are not well understood.

We have begun to explore this subject by direct measurements of cellular mechanical properties. Our approach is based on the recognition that, because cells function mechanically by changing shape, the forces that control shape must be related to the forces that drive mechanical activities. Furthermore, the forces that determine shape must resist external deformation of a cell. Therefore, we developed a method for characterizing the forces that resist cellular deformation by measuring the force required to indent the exposed surface of a cell adherent to a solid substrate (3, 4).

A method based on a similar concept was developed almost 30 years ago to measure the deformability of sea urchin ova (5). The ova were compressed by using a fine gold beam. Recently, this approach has been refined to make measurements of lipid vesicle deformability (6). Most often, cellular deformability has been studied by measuring the pressure required to aspirate a portion of the cell into a micropipette (7–9). This approach has been applied extensively to characterize the elastic properties of erythrocytes (8, 9), and some work has been done on nucleated blood cells and their precursors (10) and other types of cultured animal cells (11).

We have chosen a method based on indentation to avoid the possible detachment of the plasma membrane from the underlying cytoskeleton which might result from aspiration into a micropipette and also because of the relative simplicity in applying our method to adherent animal cells in culture. Because of the small probe tip (2 μm in diameter) and the precise sensing and control of vertical tip position (<0.1 μm), we attain excellent resolution both laterally over the cell surface and vertically in depth and rate of indentation.

In this paper we present systematic data obtained with this approach. We demonstrate that cytoplasmic and nuclear resistance to deformation is composed of both viscous and elastic components. Only cytoplasmic resistance is softened by cytochalasin B, however, which strongly suggests that it depends on the integrity of microfilaments.

MATERIALS AND METHODS

Cells. Swiss Mouse 3T3 fibroblasts (from L. Glaser, Washington University School of Medicine) were cultured in minimal essential medium (Cancer Research Center, Washington University School of Medicine) supplemented with 10% fetal calf serum (Flow Laboratories), 2% glutamine, and 1% penicillin with streptomycin (GIBCO). The cells were passaged semiweekly and were plated for experiments on 18-mm-diameter round glass coverslips at an approximate density of 10^4 cells per coverslip. These were used within 3 days.

During the measurements, the coverslip was suspended, with the cell side downward, in a specially designed, temperature-controlled chamber containing the mechanical probe (Fig. 1) immersed in about 12 ml of Higuchi medium (kindly provided by J. Baldassare, Washington University School of Medicine) buffered with 25 mM Hepes. Under these conditions the cells were viable for many hours, but generally, the experiment was terminated within the first hour.

The effects of cytochalasin B were measured on cells incubated for 1 hr at 37°C with cytochalasin B at 10 μg/ml in 1% ethanol. No cytochalasin B was present in the medium during the deformability measurements which were complete within 30 min.

The Cell Poker. The principle of the cytotensiometric measurement and a previous version of the instrument have been described (3). The details of the instrument used in these studies will be published elsewhere; the salient features are illustrated in Fig. 1. A vertical glass stylus with a tip about 2 μm in diameter mounted on a horizontal steel wire 3 cm in length is used to indent the cell. The wire is mounted on a linear piezoelectric motor. Optical sensors (MS and TS) monitor the vertical positions of the motor flag (MF) and the tip flag (TF). The cells are observed with a microscope (McBain Instruments, Chatsworth, CA) fitted with a ×32 Hoffmann modulation contrast objective and matching condenser. The experiment is con-

The publication costs of this article were defrayed in part by page charge payment. This article must therefore be hereby marked "*advertisement*" in accordance with 18 U. S. C. §1734 solely to indicate this fact.

* Present address: Department of Chemistry, University of Western Ontario, London, Canada N6A 5B7.

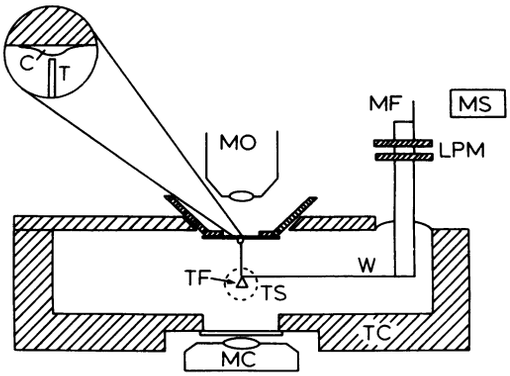

FIG. 1. Schematic representation of the cell-poking apparatus. Positioning of the cell (C) relative to the poker tip (T) is achieved by translating the top of the temperature control unit (TC) or by rotating the holder on which the coverslip is mounted. The motor assembly can be translated to ensure the tip is positioned in the field of view. W, steel wire; LPM, linear piezoelectric motor; MS and TS, optical sensors; MF, motor flag; TF, tip flag; MO, modulation contrast objective; MC, matching condenser.

tained in a gold-plated solid copper thermostatted chamber controlled to 0.1°C.

Measurements. When a varying voltage is applied to the motor, the wire undergoes a corresponding vertical displacement. The output signals of the two sensors are identical when the stylus tip is not in contact with a cell surface. When it is in contact, the force exerted on the stylus by the cell surface reduces its displacement and bends the wire slightly. By using the independently measured bending force constant, k, of the wire, it is then possible to calculate the resistive force, F, from the displacement difference, X, between the tip and the motor by $F = k \cdot X$ (3, 4). At present, a sound theoretical treatment of the elasticity of nucleated cells is lacking. We therefore have chosen to analyze and discuss the data provisionally from plots of the resistive force, F, versus the displacement, d, of the tip (3, 4).

RESULTS

Characteristics of the Cellular Response. Fig. 2 shows a typical measurement, in this case on the nucleus of a well-spread 3T3 fibroblast shown schematically in Fig. 2*B Inset*. Fig. 2*A* shows the vertical tip position as measured by the tip sensor output voltage as a function of time. The tip does not touch the cell, and the total vertical position change is 3.7 μm with a half-period of 2.5 sec (1.5 μm/sec). Curve 2 shows the output signal when the probe tip contacts the cell surface during part of the cycle. The position difference, curve 2 − curve 1, proportional to the target (cell) force, is plotted as curve 3. The force, calculated from curve 3 by using $k = 3.8$ millidynes/μm, is plotted in Fig. 2*B* as a function of tip position (zero at the horizontal line and positive values above). As indicated by the arrows, the upper trace represents the measurement going into the cell surface and the lower trace is that coming away from the cell.

Several features of this response curve are characteristic of all the measurements, although the details vary. First, prior to contact with the surface (at the extreme right of Fig. 2*B*) the cell force is zero but, as the probe deforms the surface, the force increases monotonically.

Second, the force increases nonlinearly with the depth of indentation. The deeper the indentation, the larger the apparent cell stiffness. By "stiffness," we mean the slope of the force versus indentation curve—i.e., the increase in force per unit increase in depth. In this example the stiffness increases 3-fold, from 0.75 millidyne/μm initially to 2.5 millidynes/μm. In other cases, this nonlinearity is even more pronounced.

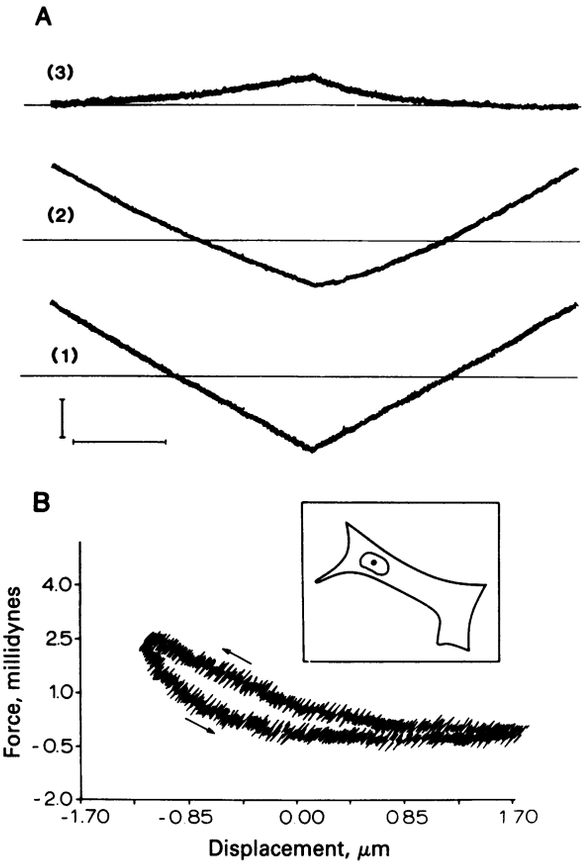

FIG. 2. (*A*) Change in vertical poker tip position as measured by the output voltage of the tip sensor as a function of time: when the tip was not in contact with a cell (curve 1) and when the tip was in contact with the cell surface during part of the cycle (curve 2). Curve 3, the difference between curves 2 and 1, measures the bending of the wire due to the cell force. The peak-to-peak amplitude is 3.7 μm and the half-period of the triangle waveform is 2.5 sec. Vertical bar, 1 μm; horizontal bar, 1 s. (*B*) The resistive force exerted by the cell as a function of vertical position of the tip, a point-by-point plot of curve 3 in *A* (scaled by a force constant $k = 3.8$ millidynes/μm) versus curve 2 in *A*. The upper trace corresponds to the descending part of curve 2 where the probe tip is moving into the cell, whereas the lower trace corresponds to the ascending part of curve 2. (*Inset*) the shape of the cell being measured and the location of the nucleus. ·, Position and relative size of the probe tip. Most of the noise in the curves arises from noise pickup in the electronics and is not representative of the true accuracy of the position control (see also Fig. 3).

Third, the force at a given position is always greater in that portion of the cycle in which the force is being increased. This hysteresis might indicate either viscoelasticity or plasticity or both.

Fourth, these adherent cells are relatively rigid. A 1-μg mass exerts a gravitational force of 1 millidyne. The corresponding pressure applied to the cell surface by the probe is about 10^{-2} atm (1 kPa) or about 100 mm H_2O. For comparison, the pressure needed in micropipette aspiration experiments on normal erythrocytes is a few millimeters of H_2O for comparable deformations (9). For osmotically swollen erythrocytes the pressures are as high as several hundred millimeters of H_2O (9); measurements on leukocytes are 10–50 mm H_2O (10).

Variability of the Measurements. The increase in stiffness with increasing depth of indentation shown in Fig. 2*B* is further illustrated in the other figures. All the available evidence (cell viability, reproducibility of responses, visual observations) indicates that the probe tip does not penetrate through or rupture

the cell membrane. Furthermore, the mechanical response of the cell to deformation depends on the position of the probe on the cell surface. This is illustrated in Fig. 3*A* which shows a series of measurements across a spread fibroblast, each beginning from the same elevation above the substrate and with the same driving amplitude. The relative positions of the probe tip on the cell are shown schematically in Fig. 3*B*. Contact with the cell surface, defined empirically by the probe height at which the force deviates measurably from zero (indicated by the arrows in Fig. 3*A*), occurred at different elevations corresponding to the different thickness of the cell body at each location. From these data it is possible to reconstruct the contour of the cell along a line joining the probe locations, shown to scale in Fig. 3*B*. An apparent systematic variation in coverslip position of about 0.3 μm over the distance from point a to point h, probably caused by drifts in the position sensors and variations in the height of the coverslip, introduces a minor uncertainty in the contour height.

In the thinner regions of the cell (points a, b, and f) the hysteresis is less pronounced. In the thick regions close to the nucleus (points c and e) the hysteresis is distinctly different from that observed on the nucleus (point d). Specifically, in the perinuclear regions the force decreased more sharply immediately after withdrawal began. This is consistent with greater viscosity or plasticity in these regions.

The initial stiffness—that is, the slope just after contact is made with the cell surface—was fairly uniform across the surface (≈0.6 millidyne/μm), but the stiffness increased more rapidly with depth on the cell body (curves c, e, and f) than on the nucleus.

Curve g illustrates the limits of detectability with our system.

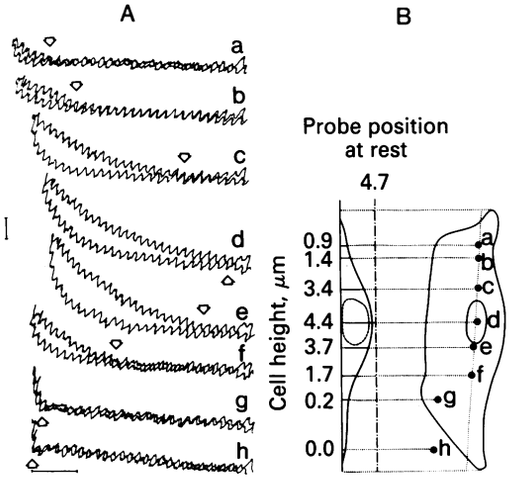

FIG. 3. (*A*) A series of compression curves similar to Fig. 2*B*. The peak-to-peak amplitude of the driving signal was 5.0 μm at a half-period of 0.5 sec. The electronic noise contribution is much more evident here because of the higher time resolution. The true noise level of the detector corresponds to the ripples on the periodic pattern. The interference has now been virtually eliminated by redesign of electronic components. Vertical bar, 1 millidyne; horizontal bar, 1 μm. Compression curves a–g represent measurements on different locations of the same cell as indicated in *B*. The rightmost point on each curve corresponds to the same elevation, 4.7 μm, above the coverslip surface (within 0.3 μm). Curve h is a measurement on the coverslip away from the cell. Arrows, elevation at which the first contact is made with the cell surface, empirically defined by the first measurable deviation of the force from zero. (*B*) Diagram of the contour of the cell used in *A*. The location of the nucleus is indicated, and the solid circles show the relative size and location of the probe tip for each of the measurements. The vertical contour of the cell is drawn to scale and is based on the elevation at which the first contact is made (arrows in *A*).

Here the cell was only about 0.2 μm thick, but the elastic response still could be detected. This is most evident when compared to the response on the coverslip surface, curve h.

Factors Affecting the Hysteresis. To investigate the hysteresis further, we varied both the rate and the amplitude of the indentation. Fig. 4 illustrates the effect of decreasing the probe velocity from 21 μm/sec (curves a and c) to 2.1 μm/sec (curves b and d) on measurements in the perinuclear region (curves a and b) and on the nucleus (curves c and d). With the slower motion, the stiffness, the net force required for indentation, and hysteresis appear to be lower in the perinuclear region. In contrast, on the nucleus, the hysteresis and the net force diminish but the stiffness is approximately independent of the velocity.

Effects of Perturbations. *Temperature.* All the measurements presented so far were performed on living fibroblasts at room temperature. The effect of raising the temperature of the system is shown in Fig. 5*A*. The largest temperature effect was observed between 33°C and 37°C, although a small change occurred between 30°C and 33°C. There were only minor changes between 30°C and room temperature (data not shown, but compare curve d of Fig. 3*A* with curve 3 of Fig. 5*A*). Interestingly, the most evident effect of raising the temperature to 37°C is to decrease the hysteresis. These curves do not correctly indicate the relative elevation of the probe. Because of thermal expansion of the chamber, sample holder, and probe assembly, the relative positions of the coverslip and probe may change by several micrometers as the temperature is varied. Therefore, we cannot be certain that the magnitude of the indentation is the same in each measurement. Nevertheless, subject to some uncertainty, it appears that the initial stiffness decreases by as much as a factor of 2 between 33°C and 37°C. A similar but less precisely documented trend was seen in the perinuclear area of the cell.

Cytochalasin B. Cytochalasin B inhibits actin polymerization and gelation *in vitro* and is presumed to disrupt the organization of microfilament structures and networks *in vivo* (12). In doses of approximately 10 μg/ml of medium it causes characteristic and pronounced morphological changes ("arborization") in adherent fibroblasts within an hour at 37°C. No morphological effects were produced by 1% ethanol, used as solvent for cytochalasin B, in the medium. The effects of this treatment on the mechanical responses are shown for two cells in Fig. 5 *B* and *C*. For comparison with an untreated cell, refer to curves c, d, and e in Fig. 3*A*. Cytochalasin B did not detectably affect measurements on nuclei (Fig. 3*A*, curve d; Fig. 5*B*, curve 2;

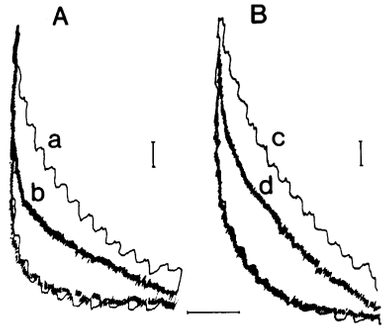

FIG. 4. (*A*) Pair of compression curves measured in the same position next to the nucleus of a cell but at different velocities. In both cases the peak-to-peak amplitude of the driving function was about 5.3 μm. The half-period was 0.25 and 2.5 sec for curves a and b, respectively. (*B*) Pair of compression curves measured in the same position on the nucleus of the same cell as in *A*. In both cases the peak-to-peak amplitude of the driving function was about 5.3 μm. The half-period was 0.25 and 2.5 sec for curves c and d, respectively. Vertical bars, 1 millidyne; horizontal bar, 1 μm.

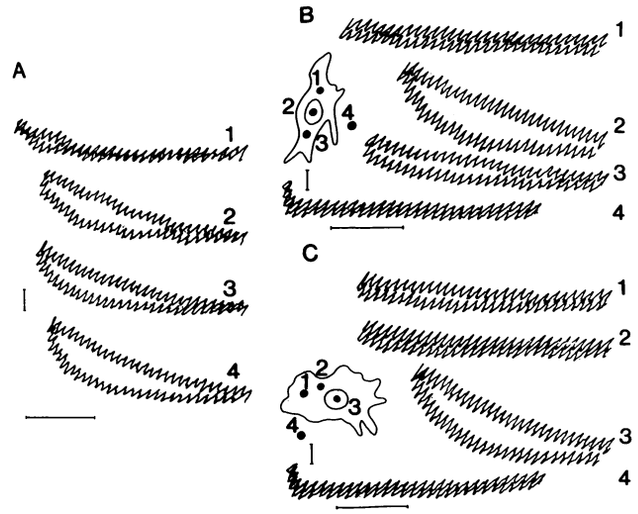

FIG. 5. (*A*) Compression curves on the nucleus of a cell at different temperatures: 1, at 37°C; 2, same cell in the same position but at 33°C; 3, different cell at 33°C; 4, same cell as in 3 in the same position but at 30°C. For comparison with a cell measured at 23°C see Fig. 3*A*, curve d. (*B*) Compression curves on a cell treated with cytochalasin B (10 μg/ml) for 1 hr at 37°C. The measurements were made at room temperature between 8 and 14 min after the cytochalasin B was washed off. (*Inset*) Arborized shape of the cell and the location of the nucleus. The positions of the measurements are indicated by the solid circles. Curve 4 represents a measurement off the cell (on the coverslip) and is correctly offset relative to curves 1, 2, and 3. (*C*) Compression curves on a cell treated with cytochalasin B (10 μg/ml) for 1 hr at 37°. These measurements were performed at room temperature between 23 and 32 min after the cytochalasin B was washed off and the cells were placed in the cell poker. Cell shape and positions of measurement were as in the *Inset*.

Fig. 5*C*, curve 3). In contrast, at points away from the nucleus, treated cells were much more deformable ("softer") than untreated cells (Fig. 3*A*, curves c and e; Fig. 5*B*, curves 1 and 3; Fig. 5*C*, curves 1 and 2). This was observed reproducibly and consistently in cytochalasin B-treated cells.

DISCUSSION

Our measurements have revealed several noteworthy characteristics of the forces by which adherent fibroblasts in culture resist local deformation. These include the large magnitude of these forces relative to those seen in erythrocytes, their hysteresis, their nonlinear increase with depth of indentation, their differences between nucleus and cytoplasm, and their temperature dependence. Our long-term goal is to explain the structural basis of these properties and their relationships to cellular physiology. The present communication is meant to be an introduction to our approach and a preliminary survey of results.

A fundamental and expected conclusion, based on the effects of cytochalasin B (Fig. 5 *B* and *C*), is that microfilaments play an important role in determining cellular mechanical properties. Interference with microfilament assembly causes 3T3 cells to change shape and to become softer. This supports our premise that measurements of deformability should characterize the forces that determine cell shape. It also indicates that both cell shape and deformability depend on the integrity of microfilaments. Although it is necessary, we cannot conclude that this integrity is sufficient for normal (i.e., unperturbed) cellular deformability. Interactions of microfilaments with other cytoplasmic structures, especially microtubules and intermediate filaments, and anchorage of filaments in the plasma membrane are also likely to be important, as are interactions with the extracellular matrix.

The striking insensitivity of the deformability of the nucleus to cytochalasin B (Fig. 5) suggests that components other than microfilaments are responsible for its mechanical properties. One possibility is that the deformability of the nucleus is determined by its contents, especially the dense matrix of interphase chromatin. It is also possible that microtubules and intermediate filaments which closely surround the nucleus play an important role (13–15). In view of the different sensitivities of nuclear and perinuclear regions to cytochalasin B, it is perhaps surprising that, otherwise, the differences in deformability between those two regions are fairly subtle. Both regions show similar magnitudes of resistance to indentation and of the hysteresis in this resistance. They differ, however, in the rate of increase of stiffness with indentation depth.

The decrease in the hysteresis with slower rates of indentation (Fig. 4) suggests viscous contributions to the cell's resistance to deformation. In some instances, however, indentation by the probe tip causes changes in the microscopic appearance of the cell which persist for relatively long periods although they eventually disappear. Persistent effects are not seen after removal of the probe tip from indentations lasting less than a few seconds, as in all measurements shown in the figures. After application of a sustained pressure of 0.1 atm or greater for several seconds, however, a circular dark spot with dimensions close to those of the probe tip is often seen with modulation contrast optics in the region of the cell to which the force was applied. The spot slowly decreases in area and disappears within a few minutes after removal of the probe. The time during which the spot remains visible depends on the magnitude and duration of the applied pressure. These visible perturbations are seen frequently in the perinuclear area but never on the nucleus and seldom in the cell periphery. Because of their persistence, these spots might result from a quasi-plastic rearrangement of cytoplasmic components in response to sustained pressure. Their mechanical properties are difficult to examine. Therefore, it is not yet clear whether or not the cell surface remains indented for some time after removal of the probe tip. Results of repeated and rapid measurements of deformability in the same location on the cell are indistinguishable, provided there is sufficient time (about a second) between withdrawal of the probe from the cell surface and resumption of contact during the subsequent measurement. Therefore the hysteresis seen in our measurements seems at least partly to have different causes (e.g., cytoplasmic viscosity) than those responsible for the persistence of quasi-plastic perturbations after sustained stress. The recovery from sustained stress is more rapid at 37°C than at 25°C. The recovery could be passive (viscoelastic) but might also be due to an active repair process of the cell related to its capability for regulated cytoskeletal rearrangement. Mitchison and Swann (7) observed a hysteresis phenomenon which they interpreted as mainly due to friction between the cell surface and the edge of the micropipette. We consider this a less likely explanation in the present experiments in part because, in contrast to a micropipette measurement, indentation does not require extensive motion of membrane in contact with an artificial surface.

The physiological significance of the hysteresis is unclear. Its diminution with increasing temperature to the extent of practically vanishing at 37°C suggests that its mechanical significance *in vivo* may be small. Nevertheless, hysteresis at lower temperatures could provide information about interactions of cytoskeletal and other cytoplasmic structures and could serve as a useful reference property for comparison of gels prepared from isolated cytoskeletal components versus authentic cellular structures. A strong dependence of deformability on temperature has also been observed in studies of leukocytes and their precursors by the micropipette method (10).

A quantitative interpretation of our measurements in terms of cellular material properties requires testing models for the observed viscoelastic behavior. We have begun by considering and eliminating simple linear viscoelastic models [composed of springs and dashpots (purely viscous components) interconnected in various series and parallel combinations]. These models cannot explain our experimental observations. All experimental plots of force, F, versus depth of indentation, z, show an upward curvature: $(d^2F/dz^2) > 0$. The linear models give downward curvatures: $(d^2F/dz^2) < 0$. It is possible that individual structural components could have linear properties but be distributed in a way that produces overall nonlinear behavior. For example, linearly elastic cytoskeletal fibers in successive mechanically independent layers at increasing depth in the cell could produce the observed upward curvature in the plots of force versus depth of indentation. A further possibility is that the cell actively readjusts its cytoskeleton to increase resistance to indentation. These models can include viscosity of a cytoskeletal gel or plasticity (e.g., due to breakage of cytoskeletal fibers), or both, to account for the observed hysteresis.

Cell models may have to include active processes, such as repair of quasi-plastic indentations and active opposition to the probe. Also, mechanical stimulation may cause a depolarization of the membrane potential. Analogous effects have been observed in neurons (16) and in fibroblasts (17). Changes in membrane potential could perturb the cytoskeleton by changing the balance of cytoplasmic ions, for example. Although these effects could complicate the analysis, they also could provide useful approaches for investigation of the control of cytoskeletal functions.

Although we cannot yet interpret our results in terms of detailed structural models, we can draw some general conclusions about the roles of plasma membrane and cytoskeleton in determining cellular deformability. The greater resistance to deformation of fibroblasts relative to erythrocytes indicates that the interwoven network of microfilaments, microtubules, and intermediate filaments which constitute the cytoskeleton of the former is capable of sustaining greater force than the spectrin-based cortical matrix of the latter. Even for erythrocytes the elasticity properties are considered to be dominated by the spectrin matrix underlying the plasma membrane rather than the membrane itself (9). We use "membrane" to refer to the lipid and integral protein components of the plasma membrane. Evans and co-workers (9) used the word to refer to the mechanical entity whose properties are measured by the aspiration technique; that "membrane" includes the actin–spectrin matrix. Hence, in the much stiffer fibroblasts we examined, the role of the plasma membrane in determining deformability is even more insignificant. This conclusion is supported by the effects of cytochalasin B and by attempts to measure the deformability of multilamellar liposomes. The latter showed undetectable resistance to deformation when a somewhat less sensitive version of our apparatus was used (3, 4).

The authors thank Mr. D. G. Lasseigne for valuable computer programming, Dr. R. Wrenn for assistance with interfacing the experiment to a VAX/VMS computer, and Dr. M. Henkart for helpful comments. This work was supported by National Institutes of Health Grants GM 21661 and GM 27160 and a grant from the Mallinckrodt Foundation. W.B.M. is supported by National Institutes of Health Training Grant 2 TB2 GM 07067-06. N.O.P. is currently a Natural Sciences and Engineering Research Council of Canada University Research Fellow. The Washington University Center for Basic Cancer Research (funded by National Institutes of Health Grant 5P30 CA 16217) provided tissue culture media.

1. Heggenes, M. H., Wang, K. & Singer, S. J. (1977) *Proc. Natl. Acad. Sci. USA* **74**, 3883–3887.
2. Albrecht-Buehler, G. (1976) in *Cell Motility*, eds. Goldman, R. D., Pollard, T. & Rosenbaum, J. (Cold Spring Harbor Laboratory, Cold Spring Harbor, NY).
3. McConnaughey, W. B. & Petersen, N. O. (1980) *Rev. Sci. Instr.* **51**, 575–580.
4. Petersen, N. O., McConnaughey, W. B. & Elson, E. L. (1981) *Comments Mol. Cell. Biophys.* **1**, 136–147.
5. Cole, K. S. (1932) *J. Cell. Comp. Physiol.* **1**, 1–9.
6. Kwok, R. & Evans, E. (1981) *Biophys. J.* **35**, 637–652.
7. Mitchison, J. M. & Swann, M. M. (1954) *J. Exp. Biol.* **31**, 443–460.
8. Rand, R. P. & Burton, A. C. (1964) *Biophys. J.* **4**, 115–135.
9. Evans, E. A. & Hochmuth, R. M. (1978) *Curr. Top. Membr. Transp.* **10**, 1–64.
10. Lichtman, M. A. (1970) *N. Engl. J. Med.* **283**, 943–948.
11. Weiss, L. & Clement, K. (1969) *Exp. Cell Res.* **58**, 379–387.
12. Spudich, J. A. & Lin, S. (1972) *Proc. Natl. Acad. Sci. USA* **69**, 442–446.
13. Osborn, M. & Weber, K. (1976) *Proc. Natl. Acad. Sci. USA* **73**, 867–871.
14. Lazarides, E. (1980) *Nature (London)* **283**, 249–255.
15. Lehto, V.-P., Virtanen, I. & Kurki, P. (1975) *Nature (London)* **272**, 175–177.
16. Julian, F. J. & Goldman, D. E. (1962) *J. Gen. Physiol.* **46**, 297–313.
17. Nelson, P. G., Peacock, J. & Minna, J. (1972) *J. Gen. Physiol.* **60**, 58–71.